Ceramics International 42 (2016) 10537–10546

Contents lists available at ScienceDirect

Ceramics International

journal homepage: www.elsevier.com/locate/ceramint

Review article

Indium doping effect on magnetocaloric, electro-transport and magnetoresistive properties of $La_{0.6}Gd_{0.1}Sr_{0.3}Mn_{1-x}In_xO_3$

K. Cherif [a,*], Arwa. Belkahla [a], J. Dhahri [a], E.K. Hlil [b]

[a] Laboratoire de la matière condensée et des nanosciences, Département de Physique, Faculté des Sciences de Monastir, 5019 Monastir, Tunisia
[b] Institut Neel, CNRS et Université Joseph Fourier, B, P, 166, 38042 Grenoble, France

ARTICLE INFO

Article history:
Received 27 February 2016
Received in revised form
21 March 2016
Accepted 26 March 2016
Available online 30 March 2016

Keywords:
Magnetocaloric effect
Model
Magnetic entropy change
Heat capacity change
Relative cooling power
Conduction mechanism
Small polaron hopping
Magnetoresistance
Percolation theory

ABSTRACT

We have investigated the influence of indium (In) doping on the structural, magneto-caloric and magneto-electrical properties of polycrystalline samples $La_{0.6}Gd_{0.1}Sr_{0.3}Mn_{1-x}In_xO_3$ ($x=0$, 0.05, 0.1), prepared by sol–gel method. The crystallographic study shows that the samples crystallize in the rhombohedric system with $R\bar{3}c$ space group. Investigations for temperature and magnetic-field dependences of magnetization indicated a gradual decrease of the ferromagnetic–paramagnetic transition temperature (T_C) from 335 to 280 K with increasing In-doping. The field dependence of magnetocaloric properties with second order phase transition material is investigated using a phenomenological model. The model parameters were determined from the magnetization data adjustment and were used to give better fits to magnetic transition and to calculate the magnetocaloric thermodynamic quantities. The magnetic entropy change reaches a peak of about 6.26 J/kg K and the relative cooling power (RCP) value of 133.36 J/kg at 325 K upon 5 T applied magnetic field for $x=0.00$. To understand the conduction mechanism, the electrical resistivity in the ferromagnetic region can be explained by electron–electron scattering process and two magnon scattering process, while that in the paramagnetic region is explained by the small polaron hopping mechanism. The maximum magnetoresistivity of 54.39% for $x=0.1$ at 5 T was obtained near room temperature 269 K.

Contents

1. Introduction

Perovskite manganite exhibits complicated interactions among electrons, lattice and spin; therefore, it has become one of the main research objects of condensed matter physics and materials physics. Especially, the finding of colossal magnetoresistance (CMR) with potential application prospect further activated people's interest for research [1,2]. However, CMR effect has the characteristics of particular temperature dependence and strong field dependence, which largely limit its application. In recent years, there has been an increasing interest in using manganites not only as a material having colossal magnetoresistivity but also

* Corresponding author.

http://dx.doi.org/10.1016/j.ceramint.2016.03.215
0272-8842/

as a material with interesting magnetocaloric properties [3–5]. In fact, the developement of new refrigeration technology, based up on the magnetocaloric effect (MCE) or electrocaloric effect has brought an alternative to the conventional gas compression technique [6, 7]. A family of Sr-doped $La_{1-x}Sr_xMnO_3$ manganites has attracted the widest interest in aspect of experimental and theoretical researches, because they exhibit the largest MCE and CMR effect [8, 9]. However, the curie temperature T_C of this material family is about 370 K, still far a way from room temperature. Fortunately, as the T_C and magnetization can be adjusted by either La-site or Mn-site doping. Soon thereafter it was demonstrated that the transition tempertaure T_C can be timed by changing either the average ionic radius of the interpolated cation or the hole doping level Mn^{3+}/Mn^{4+} ratio [10–12]. From these studies it appears that the optimization of the magnetocaloric effect properties of these materials requires the simultaneous introduction of more than three metallic elements into the perovskite matrix.

In fact, it has been revealed that these manganites, modulated by La-site substitution for example with the rare earth magnetic element Gd [13,14], have been reported to exhibit large magnetocaloric effect. However, only a few studies have been reported the doping effects at the Mn site by other elements especially non-magnetic ions. It is of much interest to know how the presence of a non-magnetic ion in the Mn-site influences the CMR and MCE properties of the material. Based on this idea, we have investigated the effect of the non-magnetic ion In^{3+} substituted in $La_{0.6}Gd_{0.1}Sr_{0.3}MnO_3$ material. In this study, we present detailed study of the structure, magnetic, magnetocaloric and magnetoresistive effect for $La_{0.6}Gd_{0.1}Sr_{0.3}Mn_{1-x}In_xO_3$ polycrystalline sample. A magnetic model described by a dependence of magnetization on the variation of temperature of this sample are presented. We used the phenomenological model to predict the values of the magnetocaloric properties from calculation of magnetization as a function of temperature under different external magnetic fields. The theoretical percolation model has been successfully used to explain the transport mechanism in the whole temperature range.

2. Experimental details

Polycristalline sample of $La_{0.6}Gd_{0.1}Sr_{0.3}Mn_{1-x}In_xO_3$ ($x=0$, 0.05, 0.1) compound is prepared by sol-gel method using metal nitrate as starting materials. This alternative preparation procedure has been developed by us for the synthesis of well-crystallized and fine-grained ferrites. In this method, the stochéometric amounts of metal nitrates in the form of solution were converted into citrates and pH was adjusted between 6.5 and 7. After getting a sol-gel by slow evaporation, a gelatin reagent, ethylene glycol was added and heated between 140 and 190°C for 12 h. Then the powder was pressed into circular pellets and finally sintered in air at 900°C for 15h. The phase purity and structure of bulk sample were identified by X-ray diffraction at room temperature using a Siemens D5000 X-ray diffractometer with a graphite monochromatized CuKα radiation (λCuKα=1.544 Å) and $20° \leq 2\theta \leq 120°$ with steps of 0.02° and a counting time of 18 s per step. According to our measurements, this system is able to detect up to a minimum of 3% of impurities. The structure refinement has been carried out by the Rietveld analysis of the X-ray powder diffraction data with FULLPROF software. The microstructure was observed by scanning electron microscope (SEM) using a Philips XL30 equipped with a field emission gun at 20 kV.

Magnetization (M) vs. Temperature (T) and magnetization vs. Magnetic field ($\mu_0 H$) were performed by using BS1 and BS2 magnetometers developed in Louis Neel Laboratory at Grenoble. The magnetic isotherms have been measured in the magnetic field range of 0–5 T. The temperature interval is fixed to 2 K in the vicinity of the Curie temperature (T_C). The temperature steps were smaller near T_C and larger further away. The resistivity measurements as a function of temperature were carried out by using the four-probe method with applying the magnetic field. The samples were cut into square shapes, with a typical dimension of 1 mm × 8 mm.

3. Results and discussion

3.1. Scanning electron microscope and X-Ray information

The detailed surface morphologies of LGSMI is determined by SEM and the corresponding image for the sample is presented in the inset of Fig. 1. From this image one can observe that the grain size and surface morphology are reasonably uniform and dense. The grain size observed by SEM (S_{MEB}) is 270–205 nm.

The average crystallite size values were also calculated using the XRD data and while doing so, instrumental errors and processing conditions were taken into consideration. The broadening of reflections due to micro-strains was considered to have an angular dependence of the form:

$$\beta_{Strain} = 4\epsilon \tan\theta$$

Where β_{Strain} is the peak shift due to strain, $\varepsilon \left(\varepsilon,=,\frac{\Delta d}{d}\right)$ is the coefficient related to strain and θ is Bragg angle. The dependence of size effect can be given by the Scherrer formula:

$$\beta_{size} = \frac{k\lambda}{S\cos\theta}$$

Where k is the grain shape factor (for a spherical grain $k=0.89$), λ is wavelength of Cukα radiation (λ=1.5406Å), S is thickness of the crystal. In the scherrer formula, β_{size} is the full width at half maxima (FWHM) of intensity vs. 2θ profile, and is defines as $\beta_{size}^2 = \beta_m^2 - \beta_S^2$. Here β_m is the experimental full width at half maximum and β_S is the FWHM of a standard silicon sample. θ is the Bragg diffraction angle of the most intense peak (104). The instrumental broadening effect has been eliminated, by subtracting the value of full width at half-maxima (FWHM) corresponding to a standard sample (SiO_2) from β_{size} at prespective Bragg peaks. The complete expression for the full width at half maximum is a

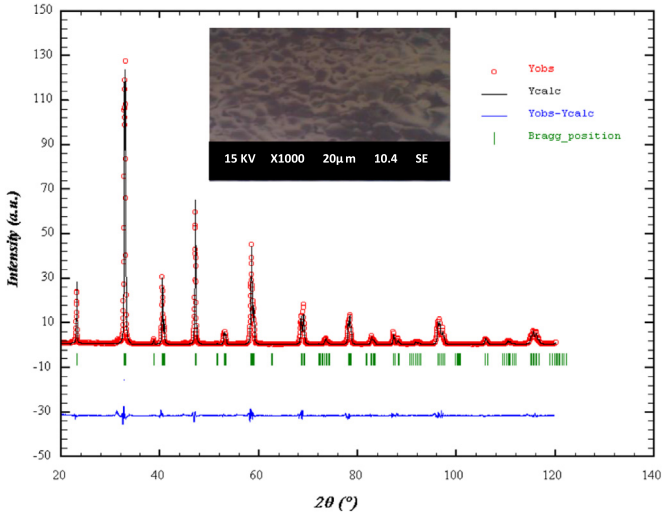

Fig. 1. Observed (open symbols) and calculated (solid lines) X-ray diffraction pattern for $La_{0.6}Gd_{0.1}Sr_{0.3}Mn_{0.95}In_{0.05}O_3$. Positions for the Bragg reflection are marked by vertical bars. Differences between the observed and the calculated intensities are shown at the bottom of the diagram. The inset represents the scanning electron micrographs showing the transect surface morphology of pellets.